Effect of Concrete Strength on GFRP-RC Circular Columns Under Simulated Seismic Loading

A. Abdallah and E. El-Salakawy

1 Introduction

The use of fibre-reinforced polymers (FRPs) in reinforced concrete (RC) structures was introduced as a solution for corrosion problems associated with presence of steel-RC members in harsh environments. However, the available codes and guidelines of steel-RC structures cannot be directly applied to FRP-RC ones. This can be attributed to the fundamental differences between each type of reinforcement. Linear elastic behaviour up to failure without yielding, relatively low stiffness and strain capacity, and different compressive and shear strengths stand out as examples of differences in behaviour of FRP with respect to steel reinforcement. Those differences, in turn, necessitated having independent design provisions for FRP-RC members. Despite having design provisions for FRP-RC structures such as ACI 440.1R-15 guidelines [2] and the Canadian code CSA/S806-12 [6], some aspects of design of FRP-RC members are still not covered or being dealt with very conservatively. For instance, FRP is not permitted to be used as main reinforcement for compression members according to the currently available ACI 440.1R-15 guidelines [2]. On the other hand, the Canadian code CSA/S806-12 [6] permits using FRP in compression members with their contribution to load carrying capacity being neglected. This can be attributed to lack of research data. Recently, there is research data proving the feasibility of using FRP as main reinforcement in compression members under different loading configurations including seismic [3, 4, 7–10]. In addition, a more recent study concluded that the currently available limit of the Canadian code CSA/S806-12 [6] for confinement reinforcement's maximum pitch of

A. Abdallah (✉) · E. El-Salakawy
Department of Civil Engineering, University of Manitoba, Winnipeg, MB, Canada
e-mail: abdalla3@myumanitoba.ca

E. El-Salakawy
e-mail: Ehab.El-Salakawy@umanitoba.ca

S. Walbridge et al. (eds.), *Proceedings of the Canadian Society of Civil Engineering Annual Conference 2021*, Lecture Notes in Civil Engineering 241,
https://doi.org/10.1007/978-981-19-0511-7_11

one-sixth the column's core diameter may seem too conservative for normal-strength concrete columns [1].

Using high-strength concrete (HSC) for RC structures is being widely spread due to the increase of load capacity it would allow, especially for compression members. The current code provisions available for design of compression members cast with HSC, especially under seismic loading, are very strict due to lack of research data. This study includes the details for preparing, casting and testing of two full-scale GFRP-RC circular columns under combined seismic and constant axial loading. The main variable was concrete compressive strength, which was 35 MPa for one specimen and 85 MPa for the other.

2 Experimental Program

2.1 Material Properties

Ready-mixed, normal-strength (NSC) and high-strength (HSC) concrete was used with a target compressive strength of 35 MPa and 80 MPa, respectively. Standard tests on 100 $\times$ 200 mm cylinders were performed to determine the actual concrete compressive strength at different ages and on column testing day [5]. The columns were reinforced longitudinally and transversally with GFRP straight bars and spirals, respectively. Table 1 includes the properties of GFRP reinforcement, as provided by the manufacture's compliance certificate.

2.2 Test Specimens

Two full-scale column-footing connections were constructed and tested. Both columns had a diameter of 350 mm and a shear span equals to 1,750 mm. The columns were reinforced longitudinally and transversally with 6-No. 16 bars and No. 10 spirals, respectively. The spiral pitch was 50 mm, in accordance with the

Table 1 Properties of GFRP reinforcement

Bar type	Bar diameter (mm)	Bar area (mm^2)	Modulus of elasticity (GPa)	Tensile strength (MPa)	Ultimate strain (%)
No. 16	15.9	197.9	65.7	1,711	2.60
No. 10 (Spirals)[a]	9.5	71.0	58.4	1,376	2.36

[a] based on tests on straight bars of the same diameter and properties

requirements of Clause 8.4.3.13 of the Canadian code CSA/S806-12 [6]. Rigid footings measured 1,400 × 900 × 600 mm were adequately reinforced with steel bars to ensure no cracking in the footings during testing. Footings were cast first, followed by casting columns as shown in Fig. 1. The details of test specimens are listed in Table 2.

Fig. 1 Casting process for test specimens

Table 2 Details of test matrix

Specimen ID	Aspect ratio (L/D)	Axial load (P/P_o)	Concrete Strength, f_c' (MPa)	Longitudinal reinforcement		Transverse reinforcement	
				Bars	ρ_F (%)	Diameter (mm)	Pitch (mm)
GN	5.0	0.2	36.0 ± 2.0	6-No. 16	1.23	9.5	50
GH		0.1	87.3 ± 2.6				

L = Shear span of the column (i.e. length of column between column-footing interface and point of horizontal load application)
D = Gross diameter of the column
P = Axial load applied on the column during testing
P_o = Theoretical unconfined axial capacity of the column
f_c' = Concrete compressive strength at age of 28 days
ρ_F = Ratio of longitudinal reinforcement to the gross area of the column

2.3 Test Setup and Procedure

All specimens were tested under simulated seismic loading accompanied by constant axial load. Horizontal actuator with 1000-kN capacity and ± 250 mm stroke length was attached to the column head to apply the horizontal cyclic loading. A large frame assembly with a hydraulic jack was used to apply the constant axial loading during testing (Fig. 2). The axial load on the two columns was similar (540 to 590 kN), which represented 20% and 10% of the theoretical unconfined axial capacity of the column for NSC and HSC specimen, respectively. The theoretical unconfined axial load capacity, P_o, was calculated according to CSA/S806-12 [6], as in Eq. 1:

$$P_o = \alpha_1 \phi_c f_c' \left(A_g - A_F\right) \tag{1}$$

where α_1 is ratio of average stress in rectangular compression block to the specified concrete strength, ϕ_c is material resistance factor for concrete, taken as unity, f_c' is specified concrete compressive strength, A_g is the gross area of concrete section and A_F is the area of FRP main reinforcement.

Test started by applying axial load on the specimen. Then, lateral load was applied with a load-controlled mode, starting with a cracking cycle followed by a service cycle. Then horizontal cyclic drifts were applied with displacement-controlled mode, as shown in Fig. 3 up to failure.

Fig. 2 Test setup

Fig. 3 Displacement history applied on the specimens

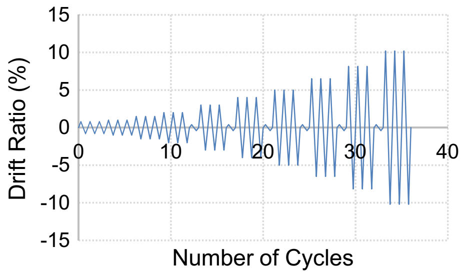

3 Results and Discussion

Figure 4 depicts the hysteretic response of the specimens. The lateral resistance of both specimens exhibited gradual increase during the early stages of loading. Specimens GN and GH, cast using NSC and HSC, reached their maximum lateral capacity of 103.5 and 111.1 kN, respectively, at 6.5% drift ratio. A second peak lateral load equals to 118 kN was reached by specimen GH at 12.75% drift ratio prior to failure. Narrow hysteresis loops with unloading portion aiming at the origin were observed, which was due to the linear elastic behaviour of GFRP reinforcement. Both specimens failed at 12.75% drift ratio, with the outermost longitudinal bar failing in compression (Fig. 5a). No spiral damage was observed for specimen GN, while spiral rupture was observed at the same location of longitudinal bar rupture for specimen GH (Fig. 5b).

As the concrete compressive strength increased from 36.9 to 87.3 MPa, with similar axial load for both specimens, the lateral load capacity increased by only 7.3%, and the drift capacity was the same for both specimens. The length of inelastic deformability hinge was similar in both columns (approximately 1.4 D). In addition, the 50 mm spiral pitch designed according to Clause 8.4.3.13 of the Canadian code CSA/S806-12 [6] was found to be too conservative for NSC columns under seismic loading with axial load level, P/P_o, of 20% and HSC column under low axial load

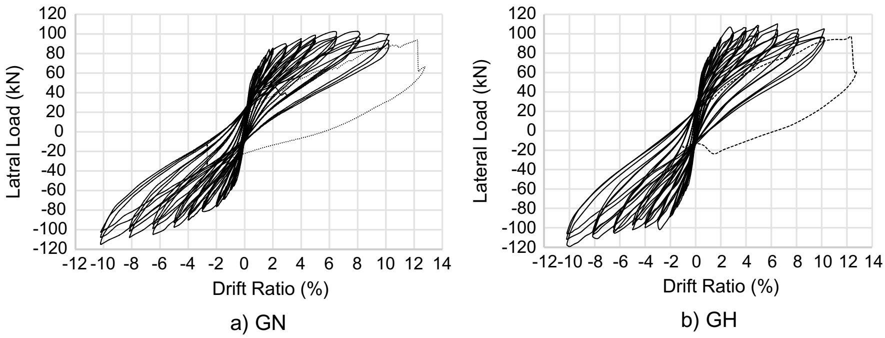

Fig. 4 Hysteretic response. **a** Specimen GN. **b** Specimen GH

a) GN b) GH

Fig. 5 Mode of failure. **a** Specimen GN. **b** Specimen GH

level ($P/P_o = 10\%$), as the actual drift ratio was 12.75%. This exceeded the 4% drift limit corresponding to ductile moment resisting frames according to the same code [6].

4 Conclusions

This paper presents the experimental results of two GFRP-RC column-footing connections tested under simulated seismic loading. One specimen was cast using normal-strength concrete, while the other was cast using high-strength concrete. The following conclusions can be drawn based upon the experimental results and discussion:

1. For well-confined columns under the same axial load value, increasing the concrete compressive strength has insignificant effect on lateral load capacity, drift capacity or inelastic deformability hinge length.
2. The requirements of Clause 8.4.3.13 of the Canadian code CSA/S806-12 [6] for confinement reinforcement pitch of FRP-RC columns seem to be too conservative for normal-strength concrete columns under seismic loading with axial load level of 20% and high-strength concrete columns with low axial load level (10%).

Acknowledgements The authors would like to express their gratitude to Natural Sciences and Engineering Research Council of Canada (NSERC) and the University of Manitoba Graduate Fellowship (UMGF) for their generous financial support. The assistance received from the technical staff at the W. R. McQuade Heavy Structures Laboratory at the University of Manitoba is greatly appreciated.

References

1. Abdallah AEM, Borgohain A, El-Salakawy E (2021) Confinement properties of GFRP-reinforced concrete circular columns under simulated seismic loading. J Compos Constr ASCE 25(2):04020088
2. ACI (2015) Guide for the design and construction of structural concrete reinforced with FRP bars. ACI440.1R-15. American Concrete Institute, Farmington Hill, Detroit, MI
3. Afifi MZ, Mohamed HM, Benmokrane B (2014) Axial capacity of circular concrete columns reinforced with GFRP bars and spirals. J Compos Constr ASCE 18(1):04013017
4. Ali MA, El-Salakawy E (2016) Seismic performance of GFRP-reinforced concrete rectangular columns. J Compos Constr ASCE 20(3):04015074, 12 pp
5. ASTM C39-18 (2018) Standard test method for compressive strength of cylindrical concrete specimens. American Society for Testing and Materials, ASTM International, West Conshohocken
6. CSA (2017) Design and construction of building structures with fibre-reinforced polymer. CSA S806-12 (R2017). Canadian Standards Association, Toronto, Ontario, Canada
7. De Luca A, Matta F, Nanni A (2010) Behavior of full-scale glass fiber-reinforced polymer reinforced concrete columns under axial load. ACI Struct J 107(5):589–596
8. Elshamandy MG, Farghaly AS, Benmokrane B (2018) Experimental behavior of glass fiber-reinforced polymer-reinforced concrete columns under lateral cyclic load. ACI Struct J 115(2):337–349
9. Naqvi S, El-Salakawy E (2017) Lap Splice in GFRP-RC Rectangular Columns Subjected to Cyclic-Reversed Loads. J Compos Constr ASCE 21(4):0401611713
10. Tavassoli A, Liu J, Sheikh S (2015) Glass fiber-reinforced polymer-reinforced circular columns under simulated seismic loads. ACI Struct J 110(6):941–951